Theoret. Chim. Acta (Berl.) 46, 205–221 (1977)

THEORETICA CHIMICA ACTA

An Open-Shell INDO Study of Models for the Stabilized O^- Ion in γ-Irradiated Alkaline Ices

Andrew T. Pudzianowski and Robert N. Schwartz

Department of Chemistry, University of Illinois at Chicago Circle, Chicago, Illinois 60680, U.S.A.

Structural models for stabilized O^- in γ-irradiated alkaline ices are evaluated. INDO calculations on hydrated O^- indicate octahedral coordination and hydrogen bond orientations for the water molecules are preferred. INDO results for hydrated OH^- are compared with crystallographic data for NaOH hydrates: a scaling factor for calculated hydrogen bond lengths is developed and applied to hydrogen bonded O^- models. The hydrated O^- model is closely similar to the hydrated anions in $KF \cdot 4H_2O$, $NaOH \cdot 4H_2O$, and $NaOH \cdot 7H_2O$. A second model is developed, involving H_3O^+ along with H_2O, in the O^- stabilization shell. Both models are discussed in terms of alkaline ice radiation chemistry.

Key words: O^- ion in irradiated alkaline ice

1. Introduction

The O^- ion is one of the two principal paramagnetic species (the other being the stabilized, or "trapped" electron) observed in concentrated aqueous NaOH ices which have been gamma-irradiated at low temperatures. (Comprehensive reviews of the radiation chemistry in these systems have been made by Kevan [1, 2]. Experimental results cited here are from these sources unless otherwise specified.) The solid matrix is assumed to be a disordered glassy system at 77°K, and if it is left undisturbed both species are stable and long-lived. Hence, both have been studied extensively via electron paramagnetic resonance (EPR) methods; however, the O^- signal is partially obscured by that of the trapped electron, and hence information regarding the nature of the latter has been easier to extract. It is only very recently [3] that the hitherto assumed assignment of the O^- signal has been shown to be correct, through analysis of its hyperfine structure in ^{17}O enriched alkaline ice.

There has, in addition, been some work done with gamma-irradiated NaOH crystalline hydrates [4] at low temperatures, which helps shed some light on how the degree of ordering influences the stabilization of the principle products in such systems. In $NaOH \cdot 3.5H_2O$, for example, the radiation chemical yield for trapped electrons is some forty times lower than in glassy NaOH ice, and while no quantitative yield is given for O^- its presence is nonetheless reported.

A detailed picture of the structural aspects of electron stabilization in glassy NaOH ices was recently arrived at [5], using both lineshape analysis of the trapped electron EPR signal in an ^{17}O enriched matrix and spin echo techniques. While such detailed information is not yet available for O^- ion in the same systems, it appears likely that some combination of EPR and related methods, especially electron spin echo, will supply this information in the near future. We therefore have a timely opportunity to test existing theoretical methods of evaluation of structural models for stabilization.

In general, it would be fair to say that product stabilization is a central problem in radiation chemistry. The energies available at the outset are generally so large as to dwarf those involved in ordinary chemical reactions, but products will not be observed unless they can somehow be stabilized. There is, in addition, the problem of complexity to contend with: a chemical system under irradiation may simultaneously feature direct radiolysis reactions, reactions involving secondary radiation particles which have been produced by scattering, and reactions involving transient chemical species which are not directly observable. Hence, for such products as are observable it is important to identify the nature of their stabilization, since this information may help clarify the mechanisms by which they are formed.

With these considerations in mind, then, the present authors developed a number of hypothetical models for O^- stabilization in an aqueous matrix. In this paper we report the results of a theoretical evaluation of these models and initiate discussion of some of their implications. More extensive considerations have been deferred to subsequent work, currently in progress, and we hope that the rather detailed structural models described here will serve to stimulate further discussion of the radiation chemistry in alkaline ice systems.

2. Approach, Calculations, and Models

2.1. Overall Approach

The general approach we take here is based on the "supermolecule" formalism current in solvation theory at the molecular level, in which the "solute-solvent" aggregate is considered as one large molecule to which existing methods of analysis are to be applied. (Comprehensive reviews are available [6, 7] which provide assessment of solvation and hydration theory.)

The effects of species other than the nearest neighbors of the O^- ion assumed in our models have not been included in any explicit way, and so our treatment is formally a "gas phase" approach in terms of the supermolecule. On the other hand, our

choice of structural models has been influenced quite a bit by experimental results for F^- and OH^-, as will be related presently.

The calculations employed the INDO formalism in both open and closed shell form [8]. The choice of this formalism could be considered from several viewpoints, but our main concern was the examination of trends among related species, which is the type of situation in which neglect of different overlap (NDO) theories have been most effective. We are, of course, aware that NDO theories have shown some deficiencies when it comes to anion hydration [6, 7], and have commented in the Discussion on how these manifest themselves in our results. We have reported and attempted to evaluate numerical results wherever these seemed relevant. In particular, it may be important to have some idea of how various proposed models for O^- stabilization differ regarding spin density distribution. INDO results along these lines have been shown capable [8] of at least semi-quantitative agreement with experiment. Finally, the relative CNDO/2 formalism has had fairly extensive application to the study of anion hydration [9–12], so there are grounds for comparison from that direction.

2.2. Structural Models

The structural models for O^- stabilization are shown in Figs. 1 and 2. Those in Fig. 1 imply stabilization provided entirely by hydration, and thus are superficially analogous to hydration models for singlet ground state anions. The coordination of water molecules about the central O^- is restricted to tetrahedral and octahedral, because these two types appear to represent the extremes in aqueous media. That is, hydrogen bonding in pure water and its ices appears to follow tetrahedral arrangements under normal conditions; on the other hand, the preferred coordination of water molecules about the anion in the crystalline hydrates $NaOH \cdot 4H_2O$, $NaOH \cdot 7H_2O$, and $KF \cdot 4H_2O$ is octahedral [13]. The actual orientation of the waters was likewise restricted to two cases: hydrogen bond (T-I and O-I), and dipole (T-II and O-II). These are mixed in models T-III and O-III.

The models involving O^- in Fig. 2 reflect the intuitive idea that models for O^- stabilization in a relatively rigid aqueous matrix might profitably be patterned after the structural aspects of OH^- hydration, since the latter anion is most probably the chemical precursor of O^- in irradiated alkaline ice [1, 2]. Thus, hydrated OH^- may provide a "built-in" trapping site for the product O^-, so we also examined the hydrogen bonded models for OH^- shown in Fig. 2.

2.3. Open Shell Formalism

A detailed exposition of open shell molecular orbital theory is given by Pople and Beveridge [8]. We therefore restrict our comments to those aspects which are directly relevant to the calculated results we report. The notation throughout is that of Pople and Beveridge.

The description of electron density, and the related properties of spin and charge density, begins with the formulation of independent density matrices, defined in

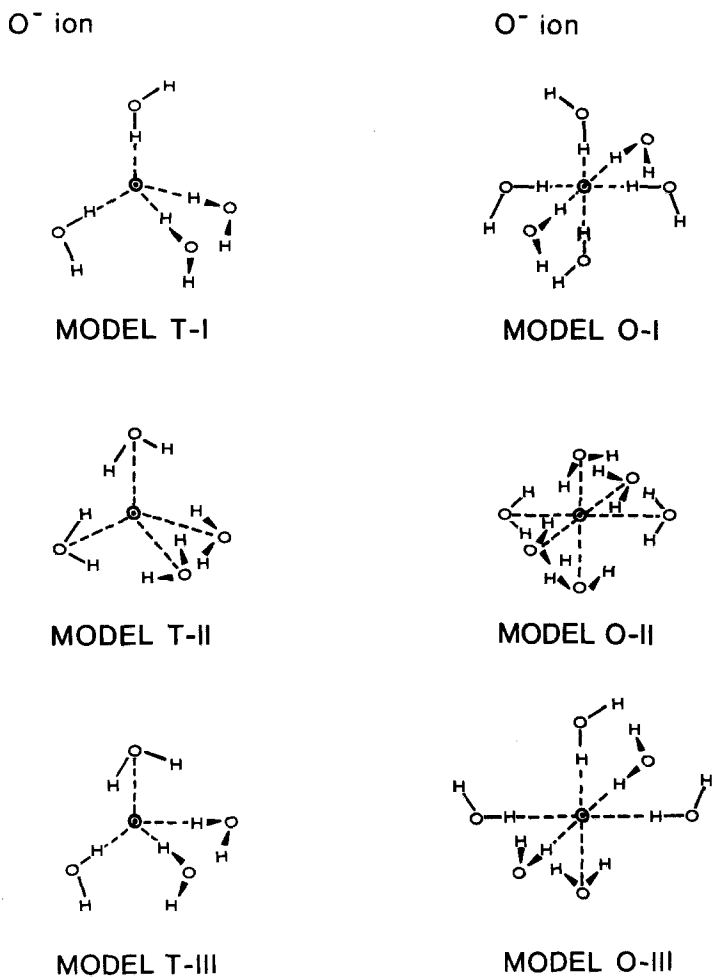

Fig. 1. Structural models for hydrated O^- ion

terms of their elements as

$$P^{\alpha}_{\mu\nu} = \sum_{i}^{p} C^{\alpha}_{\mu i} C^{\alpha}_{\nu i}, \qquad P^{\beta}_{\mu\nu} = \sum_{i}^{q} C^{\beta}_{\mu i} C^{\beta}_{\nu i}. \tag{1}$$

Here the C's are expansion coefficients on basis atomic orbitals in the i'th molecular orbital, the subscripts μ, ν distinguish between the basis orbitals, and there are p electrons of α spin and q electrons of β spin. The sum of these matrices is the total SCF density matrix, and the diagonal elements of this latter give the distribution of electron population over the various atomic centers. Each atom contributes a block along the diagonal corresponding to its allotted basis functions, and the sum of the diagonal elements in each such block gives the valence electron population (VEP) for the atom in question.

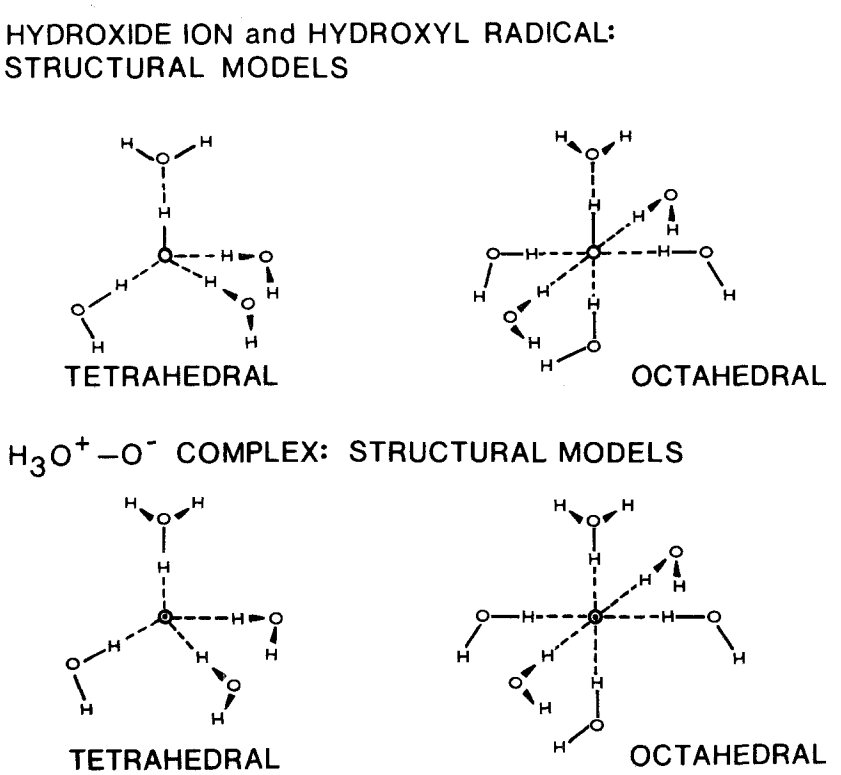

Fig. 2. Structural models for hydrogen bonded OH^- and OH radical, and for $H_3O^+-O^-$ complexes

The spin density distribution is derived from the difference between the α and β density matrices, in terms of the quantity

$$\rho_{\mu\nu}^{\text{spin}} = P_{\mu\nu}^{\alpha} - P_{\mu\nu}^{\beta}. \tag{2}$$

This quantity is properly a spin population, although it is often termed a "density". The spin population on an atom-by-atom basis is derived in the same manner as the VEP just described.

The theoretical expression for the isotropic hyperfine coupling constant a_n for atom n relates this constant to the s-orbital spin density on that atom. However, the Slater basis used in INDO calculations is unsuitable for theoretical evaluation of the spin density by direct calculation [8], so Pople and coworkers have expressed the relation between a_n and the s-orbital spin population in the linear form

$$a_n = m\rho_{sn,sn}^{\text{spin}} \quad , \tag{3}$$

where m is determined from the best least squares fit between observed coupling constants and calculated s-orbital spin populations for various atoms. The results are given in Pople and Beveridge [8], and have been incorporated in open shell INDO computer programs.

2.4. *Optimization of Geometries*

The discrete molecular species involved in our structural models were held fixed, throughout, at their INDO optimum geometries [8]. The bond lengths and angles are given in Table 1, along with the corresponding INDO total energies. (The parameters for H_3O^+ were determined from our own closed shell calculation.)

Table 1. INDO Optimum geometries and total energies for component species[a]

Species	O–H Bond (Å)	H–O–H Angle (°)	−E (Total) (a.u.)
O^-	—	—	17.19238
OH^-	1.100	—	18.07167
OH	1.033	—	18.16253
H_2O (C_{2v})	1.030	104.7	19.03935
H_3O^+ (C_{3v})	1.050	117.0	19.46802

[a] Units used are as follows: 1 Å = 10^{-10} m, 1 a.u. (Hartree) = 4.35981 aJ, 1 kcal = 4.184 kJ, 1 G (Gauss) = 10^{-4} T (tesla).

The models in Fig. 1 all have the O^- at the origin of coordinates. In the tetrahedral models water oxygens are at the corners of a tetrahedron, while in the octahedral models these lie along the positive and negative coordinate axes. All hydrogen bonded waters in Fig. 1 are in "donor" orientations, while the orientation in the remaining models (Fig. 2) should be clear.

Optimum geometries were arrived at by systematically moving the stabilization shell molecules with respect to the origin, in steps of 0.1 Å, along the lines between their oxygens and the origin. Rotation about these lines had very little effect on the total energies except in the all-dipole models T-II and O-II, where the hydrogens on adjacent molecules crowded each other in some orientations.

The optimized geometries for all models are summarized in Tables 2 and 3. These are given in terms of R(O–O), the distance between a stabilization shell oxygen and the central oxygen in each model. In all cases there is a set of equal distances: these pertain only to water molecules and are designated as "equiv" in the tables, while the number of instances is given in parentheses. The remaining distances are designated "nonequiv" and further information is given in parentheses.

Calculations of atomic coordinates and INDO calculations were performed, respectively, using modified versions of the Fortran programs MBLD and CNINDO [14].

Table 2. Optimized geometries and total energies for hydrated O^- models

Structural model	R(O–O) (Å) Equiv	R(O–O) (Å) Nonequiv	−E (Total) (a.u.)
T-I tetrahedral all H-bond	2.4000 (3)	2.3000	93.63532
T-II tetrahedral all dipole	2.2000 (3)	1.9000	93.50660
T-III tetrahedral mixed	2.4000 (3)	1.9000	93.63008
O-I octahedral all H-bond	2.4000 (6)	— —	131.77336
O-II octahedral all dipole	2.2000 (5)	2.3000	131.64780
O-III octahedral mixed	2.4000 (4)	2.2000 2.3000	131.76450

Table 3. Optimized geometries and total energies for all hydrogen bonded models

Model	R(O–O) (Å) Equiv	R(O–O) (Å) Nonequiv	Scaled R(O–O) (Å) Equiv	Scaled R(O–O) (Å) Nonequiv	−E (Total) (a.u.)	Scaled −E (Total) (a.u.)
O^- T-I	2.4000 (3)	2.3000	2.7000	2.5875	93.63532	93.55632
O^- O-I	2.4000 (6)	—	2.7000	—	131.77336	131.69379
OH^- Tetrahedral	2.3000 (3)	2.6000	2.5875	2.9250	94.46338	94.41371
OH^- Octahedral	2.4000 (5)	2.6000	2.7000	2.9250	132.60798	132.52960
OH Tetrahedral	2.5000 (3)	2.4000	2.8125	2.7000	94.40674	94.37150
OH Octahedral	2.5000 (5)	2.4000	2.8125	2.7000	132.50755	132.46848
H_3O^+–O^- Tetrahedral	2.4000 (3)	2.2000 (H_3O^+)	2.7000	2.4750	94.36385	94.28387
H_3O^+–O^- Octahedral	2.5000 (5)	2.2000 (H_3O^+)	2.8125	2.4750	132.47428	132.38031

2.5. *Scaling of Optimized Geometries*

Our optimized structures for hydrated OH^- were compared with crystallographic data for the hydrates $NaOH \cdot 4H_2O$ and $NaOH \cdot 7H_2O$ [13]. In the tetrahydrate the OH^- has six nearest neighbor water molecules arrayed in a distorted octahedron about the central anion. Five of these are at R(O–O) distances of 2.68–2.73 Å, while the sixth is at 3.11 Å. The situation in the heptahydrate is similar: five water oxygens are at distances from 2.50 Å to 2.93 Å and a sixth is at 3.15 Å. These arrangements are interpreted [13] as corresponding to five strong hydrogen bonds, with hydroxide oxygen as acceptor, and a sixth weaker hydrogen bond with the hydroxide O–H bond as donor.

The acceptor bonds in our octahedral OH^- are characterized by R(O–O) = 2.40 Å. We took 2.70 Å as a likely figure, as suggested by the hydrate data above, and treated the ratio 2.70/2.40 = 1.125 as a "scaling" factor, by which all our calculated hydrogen bond lengths would be multiplied to bring them more in line with the empirical model.

This adjustment was made to all our optimized hydrogen bonded models, and the appropriate open or closed shell calculation was repeated at the new coordinates. The outcome in each case is given in Table 3, where the new results are given as "scaled".

Table 4. Interaction energies for all hydrogen bonded models

Model	$-\sum E_i$ (a.u.)	$-\Delta E$ (a.u.)	$-\Delta E$ (kcal/mole)	Scaled $-\Delta E$ (a.u.)	Scaled $-\Delta E$ (kcal/mole)	OH^- Shell[a] $-\Delta E$ (a.u.)	OH^- Shell $-\Delta E$ (kcal/mole)
O^- T-I	93.34978	0.28554	179	0.20654	130		
O^- O-I	131.42848	0.34488	216	0.26531	166		
OH^- Tetrahedral	94.22907	0.23431	147	0.18464	116		
OH^- Octahedral	132.30777	0.30021	188	0.22183	139		
OH Tetrahedral	94.31993	0.08681	55	0.05157	32		
OH Octahedral	132.39863	0.10892	68	0.06985	44		
H_3O^+–O^- Tetrahedral	93.77845	0.58540	367	0.50542	317	0.42872	269
H_3O^+–O^-	131.85715	0.61713	387	0.52316	328	0.44859	282

[a] These results are derived from the following total energies: tetrahedral −94.20717 a.u., octahedral −132.30574 a.u.

2.6. Interaction Energies

The interaction energy for a supermolecule is analogous to the binding energy in an ordinary molecule, in that it is a measure of the tendency of the component molecular and ionic species to hold together in an aggregate. Pursuing the analogy, then, we can define this interaction energy as follows:

$$\Delta E = E - \sum_i E_i . \tag{4}$$

Here E is the total energy of the supermolecule and the E_i are the total energies of the component molecules and ions.

Calculated interaction energies for all hydrogen bonded models are assembled in Table 4, where they are given for both the INDO optimum geometries and the corresponding scaled geometries.

The interaction energies correspond to hydration in all but the H_3O^+–O^- models, where the ΔE may be partitioned into a hydration contribution and a contribution from the interaction of the two ions. To evaluate these we carried out separate calculations on fragments, consisting of the H_3O^+ and O^- ions without the water molecules of the complete aggregate, in which the spatial relationship between the ions is exactly the same as in the aggregates. The calculations would not converge (as in CNDO/2 calculations on hydrogen bonded H_3O^+ and NO_3^- [15]), so we modified the CNINDO program to incorporate the density matrix averaging procedure suggested by Chesnut and Wormer [16]. The ΔE contribution due to the ions was then extracted from the total energies of the fragments, through use of Eq. (4).

2.7. Additional Calculations

The two H_3O^+–O^- models were also examined at R(O–O)'s equal to those for the corresponding scaled OH^- models, in view of the close relation proposed earlier for these. Results are given as "OH^- shell" along with other H_3O^+–O^- results in the tables.

For comparison with the H_3O^+–O^- models, calculations were also carried out on hydrated OH radical, as the supermolecules with corresponding coordination (Fig. 2) have the same complements of atoms and electrons, and therefore the same overall neutral charge and doublet ground state.

Finally, we examined an octahedrally coordinated O^- model analogous to O-II (Fig. 1), but with the O–H bonds of all waters pointing away from the central oxygen. The motivation and results for this calculation are discussed further on, in Sect. 4.4.

3. Results

Numerical results basic to comparative evaluation of the models are assembled in Tables 1 through 4.

On the basis of ΔE values (Table 4), octahedral coordination is preferred over tetrahedral in all cases. Of the hydrated O^- models in Fig. 1, model O-I is the preferred structure. In summary, octahedral coordination with hydrogen bonding is the most favorable situation for the hydrated O^-.

In the H_3O^+–O^- models (Fig. 2), partitioning of ΔE's showed that their large values are due mainly to the single interaction between the two ions. This contribution is as follows: unscaled, −314 kcal/mole; scaled, −209 kcal/mole; OH^- shell, −155 kcal/mole.

Finally, it should be noted that on the basis of total energy, the hydrated OH radical is more stable than the H_3O^+–O^- supermolecule in both the unscaled and scaled cases. This is to be distinguished from the greater stabilization (ΔE) provided to the radical species by the latter supermolecule.

4. Discussion

In order to establish some perspective for the O^- models discussed here, we have had to draw for the most part on theoretical and experimental results for chemically related anions. These considerations seem to establish the qualitative similarity, naively expected, between the anions O^-, F^-, and OH^-. (The point is considered further in Sect. 4.4.) We have also considered the EPR results available for ^{17}O enriched alkaline ice [3] in terms of our results, but we must recognize at the outset that the ground here is probably less firm. Both types of comparison serve to establish what may be expected of an INDO approach in quantitative terms, and we have attempted to evaluate this aspect wherever possible. Finally, we have tried to establish how the O^- models fit into the overall context outlined in the Introduction.

4.1. Hydrated O^- *Models*

Models T-I and O-I (Fig. 1) were evaluated by comparison with available information concerning F^- and OH^- hydration.

CNDO/2 calculations involving F^- hydration [10] give optimum O–F distances of 2.382 Å and 2.443 Å, respectively, for hydrogen bonded tetrahedral and octahedral coordination. The optimized (unscaled) R(O–O) values for models T-I and O-I (Table 2) are in excellent agreement with these figures.

Crystallographic results for the hydrate $KF \cdot 4H_2O$ [13] should provide a good empirical model for O^- in a solid aqueous matrix. Each F^- has a first coordination shell of six water molecules in an octahedral array, with O–F distances of 2.71–2.78 Å. The scaled model O-I (Table 3) is in excellent agreement with these results.

For the calculated hydration energies, the agreement between our O^- results (Table 4) and CNDO/2 F^- results [10] is also suggestive. The latter values are −164 and −190 kcal/mole, respectively, for the tetrahedral and octahedral cases.

These calculated results may be compared most directly with experimental heats of hydration for F^- in the gas phase [17], which extend directly to clustering of F^- with five water molecules. One can readily project a value of about -93 kcal/mole for six waters, while the experimental value for four is -67.1 kcal/mole. Thus, the reported CNDO/2 hydration energies for the tetrahedral and octahedral cases are overestimated by 144% and 104%, respectively.

Our OH^- hydration results furnish an example of this overestimation by the INDO procedure. Analogous gas phase hydration studies of OH^- [18] lead to heats of hydration closely similar to the F^- results: -68.2 kcal/mole for four and a projected -95 kcal/mole for six waters. The unscaled INDO results for OH^- are therefore overestimated by 115% and 98% for the corresponding cases, while scaling the hydrogen bond lengths brings this down to 70% and 46%. We may assume that our results for the scaled models T-I and O-I are overestimated by roughly these last two figures. (We note that the tendency of NDO theories to exaggerate interactions in anion hydration studies has been commented on elsewhere [7].)

This tendency also appears in the calculated valence electron populations (Table 5), especially for the central oxygen, nominally an O^- ion with seven valence electrons. While the amount of electron density transferred to the waters does not seem excessive (INDO VEP's for free water: 6.31 oxygen, 0.84 each hydrogen), the central oxygen does donate electron density to the off-diagonal elements of the bond order matrices (Eq. 1) to a greater extent that might be expected, thus building up the strength of the hydrogen bonds.

These same VEP results (Table 5) imply axial symmetry, about the x-axis, in terms of the charge distributions for the water oxygens and the nearest-neighbor hydrogens to the O^-. We might note that this symmetry is very nearly octahedral.

4.2. H_3O^+–O^- *Models*

The existence of hydrogen bonded complexes of the type H_3O^+–X^- is indicated by detailed experimental results for acid monohydrates $HX \cdot H_2O$. (A summary of such information is given in [15].) Our calculated parameters for free H_3O^+ (Table 1) are quite comparable to experimental geometries for the complexed cation, but the optimized H_3O^+–O^- distances (Table 3) are short by comparison with experimental H_3O^+–X^- distances ($\sim$2.6–2.95 Å), even after scaling. This would indicate that the interaction between the cation and anion has been overestimated even more than those between O^- and neutral H_2O, as exemplified by our hydrated O^- calculations.

The degree of overestimation is clearly indicated by the large ΔE obtained for the single H_3O^+–O^- interaction, which amounts to -155 kcal/mole even for the largest separation examined (2.90 Å). We can see that introduction of a cationic species intensifies the problem of overestimation, already present for anion–neutral molecule interactions.

Table 5. Valence electron populations (VEP) and isotropic hyperfine coupling constants for O^- and nearest neighbors[a]

Model O-I (scaled)

Atom	O(origin)	O(x, $-x$)	O(y, $-y$)	O(z, $-z$)	H(x, $-x$)	H(y, $-y$)	H(z, $-z$)
VEP	6.68	6.37, 6.37	6.40, 6.40	6.40, 6.40	0.77 (all)		
$a^{(Gauss)}$	−6.60	−1.75, −1.75	0.57, 0.60	0.56, 0.62	−23.5, −23.5	1.04, 1.02	1.04, 1.02

H_3O^+–O^- (scaled) octahedral

Atom	O(origin)	O(x, $-x$)	O(y, $-y$)	O(z, $-z$)	H(x, $-x$)	H(y, $-y$)	H(z, $-z$)
VEP	6.51	6.34, 6.35	6.36, 6.36	6.22, 6.36	0.82, 0.82	0.81, 0.81	0.71, 0.81
$a^{(Gauss)}$	−8.90	−0.07, −0.18	0.20, 0.21	19.6, 0.20	−17.5, −17.3	1.10, 1.10	−32.1, −0.52

H_3O^+–O^- (OH^- shell) octahedral

Atom	O(origin)	O(x, $-x$)	O(y, $-y$)	O(z, $-z$)	H(x, $-x$)	H(y, $-y$)	H(z, $-z$)
VEP	6.49	6.35, 6.36	6.38, 6.38	6.17, 6.37	0.81, 0.81	0.80, 0.80	0.76, 0.80
$a^{(Gauss)}$	−7.25	−0.32, −0.36	0.40, 0.41	56.5, 0.75	−25.5, −25.5	1.89, 1.90	−84.7, −5.37

[a] Atoms are specified as lying along the positive and negative axes in parentheses.

As in model O-I, the exaggeration manifests itself most strongly in the calculated VEP of the central oxygen (Table 5), which now only has a nominal charge of -0.5. (INDO VEP's for free H_3O^+ : 6.14 oxygen, 0.62 each hydrogen.)

The symmetry with respect to nearest-neighbor charge distribution here is very nearly axial, with the z-axis being singled out this time, but we note that regular octahedral symmetry is not approached. The difference between the two models for O^- stabilization is reflected in the calculated isotropic hyperfine coupling constants (Table 5): qualitatively, the H_3O^+–O^- model features relatively large splittings from three nearest-neighbor hydrogens, whereas only two such splittings are associated with model O-I.

4.3. EPR Results for O^- in Alkaline Ice

The work on ^{17}O enriched alkaline ice by Schlick and Kevan [3] provides the only information available for oxygen hyperfine coupling in this type of system. Even so, these workers were able to determine directly only the parallel component of the hyperfine coupling. However, by assuming the spin density to be localized in a $2p$ orbital on the O^- and selecting a likely value for the dipolar contribution to the hyperfine tensor, they proceeded with the calculation of the isotropic splitting and the $2p$ spin density. This was done through the use of an empirical equation deduced for π-radicals, which implies a linear relation between the isotropic splitting constant and the $2p$ spin population on the same atom [3]. The values obtained are, respectively, -28G and 0.69 for the isotropic coupling and the $2p$ spin population.

These values may be compared directly with results deriving from our models. The coupling constants for the central oxygen (Table 5) are nearly the same for both O^- models, and are negative. This last implies positive s-orbital spin populations on this oxygen, as the equation (3) proportionality constant for ^{17}O is negative [8]. The INDO $2p$ spin population results are also similar for both models, being about 0.95 for the $2p_x$ orbital of the central oxygen in both cases. Thus, the INDO results confine virtually all the positive spin density (α-spin) to an "O^-" $2p$ orbital, in agreement with the initial assumption used by Schlick and Kevan to analyze their results.

However, it does seem that the calculated value for the $2p$ spin population obtained by these workers is too small, probably because of the π-radical relation used to obtain it, which *a priori* implies more delocalization of positive spin density than seems appropriate for a hydrated species. In any event, the result itself is not entirely consistent with the initial assumption of confinement of the unpaired spin density to a $2p$ O^- orbital. We again note that this latter condition is obtained as a *result* in our calculations, which give the same conclusion for two somewhat different O^- environments.

4.4 Anion Character of O^- in Alkaline Ice Systems

Before discussing the relation between our structural models and radiation chemistry, we offer some preliminary comments on a point which we propose to

examine in greater detail elsewhere. It has been suggested [19] that O^- may behave like a cation as regards hydration. This idea is a consequence of the "hole" formalism, which has been applied (though to a limited extent) to the analysis of EPR results for O^- in alkaline ice [3]. It has been successfully used, in modified and extended forms, as a description of the O^- ion in solid oxides, e.g., MgO [20], which have been radiation-damaged or otherwise altered so as to produce paramagnetic centers. Thus, in such highly ordered systems O^- is thought of as an electron-deficient O^{-2} site in the lattice, or as a "hole" trapped on an O^{-2} site, which is then analyzed in terms of the surrounding ions and the resulting crystal field [20].

Without going into too much detail, we might suggest that alkaline ice systems are properly thought of as molecular solids with ionic impurities. The ion-molecule interactions are weak on the chemical scale and, again assuming the crystalline hydrates as valid empirical models, all ions have a first coordination shell of water molecules, so there is no direct interaction among atomic ions. This is in marked contrast to the situation in ionic solids like alkaline-earth oxides, where a crystal field approach serves well.

A second, more specific consideration is the following. An O^- ion at a site normally occupied by O^{-2}, as in a solid oxide, represents a situation in which one negative charge is "missing" locally, and hence such a site is formally a cation vacancy. However, proposed mechanisms for the formation of O^- in alkaline ice [1, 2] involve OH^- as the parent species, so the net effect is the local replacement of OH^- by O^-. Hence, a hydrated O^- ion, regardless of the water molecule orientations, has the same overall charge as a hydrated OH^- ion: there is no missing charge locally, and there is no cation vacancy.

Finally, we consider the similarity between O^- results and those for analogously hydrated OH^- and F^-, as outlined in Sect. 4.1 above, as compelling evidence for the anion character of O^- in an aqueous environment. However, since it might be argued that this is a consequence of the orientation of waters in the O^- structural models, we now briefly consider results we obtained for a "cation" orientation of the water molecules. This is the model described in the last paragraph of 2.7, above.

The INDO optimized geometry here was a structure with R(O–O), defined as before, equal to about 1.4 Å for all six waters, a total energy about 0.10 a.u. (63 kcal/mole) more stable than the unscaled model O-I, and a resulting ΔE more stable by the same amount. While the overall charge is -1, there is no O^- in this structure, the VEP for the central oxygen being 5.89, i.e., slightly more positive than a neutral oxygen. The $2p$ spin population for this atom is 0.47, the $2p$ orbital accounting for 0.42 of this, and the s-orbital spin population is very small and *negative*, implying a positive coupling constant.

The anomalous character of some of these results, particularly the very short R(O–O)'s, can probably be attributed to the way electron–electron repulsions are handled in an INDO calculation. These are evaluated explicitly only over Slater

s-functions [8], and thus might be expected to underestimate repulsions between sizable groups of atoms with nearly full *p*-subshells. In connection with this, we note that for $R(O\text{–}O) = 2.40$ Å, as in the unscaled model O-I, the total energy for this "cation" O^- model is 0.41 a.u. (260 kcal/mole) *less* stable than model O-I. In fact, the energy does not become more negative than the optimum value for model O-I, until $R(O\text{–}O)$ for this "cation" model goes below 1.6 Å. We also noted the rapid loss of VEP for the central oxygen as $R(O\text{–}O)$ decreased from around 2.4 Å, where there was initially a well-defined O^- ion.

Thus, if we keep in mind the particular shortcoming of the INDO procedure mentioned above, the calculation cannot be said to support the full extension of the "hole" formalism to alkaline ice systems. Instead, we feel that these results, taken in context with the considerations outlined earlier in this section, tend to establish the anion character of O^- in these molecular systems.

4.5. O^- Models and Radiation Chemistry of Alkaline Ice

In the alkaline ice irradiation described in the introduction, the O^- ion is thought to be produced by reaction of OH radical with hydroxide ion, and the following two mechanisms have been proposed [1, 2]:

$$\begin{aligned} H_2O &\rightsquigarrow H_2O^+ + e^- \\ H_2O^+ + H_2O &\longrightarrow H_3O^+ + OH \\ OH + OH^- &\longrightarrow H_2O + O^- \end{aligned} \tag{5}$$

and

$$\begin{aligned} OH^- &\rightsquigarrow OH + e^- \\ OH + OH^- &\longrightarrow H_2O + O^-. \end{aligned} \tag{6}$$

The ionization steps are believed to be carried out by low-energy secondary electrons rather than directly by radiation. The final step in each mechanism is consistent with the decrease in trapped OH yield observed as initial OH^- concentration is increased. The reactions, of course, imply the proximity of the two reacting species, which poses no problem in a liquid medium. However, restricted translational motion in the solid state would seem to require that hydroxyl radicals be produced close to hydrated OH^- ions, a condition which must effectively be met both by molecular structural descriptions and by proposed reaction mechanisms. We now ask how mechanisms (5) and (6) and our proposed structural models are related.

We begin with our octahedral model for OH^- hydration, in which the scaled distances correspond well to the crystallographic results for $NaOH \cdot 4H_2O$ and $NaOH \cdot 7H_2O$. If we accept restricted translational motion at 77°K and below as a valid condition, we find that the entire sequence of reactions (5) can take place, step for step, within the first coordination shell of a hydrated OH^- ion. The overall effect of mechanism (5) would then be the conversion of octahedrally hydrated OH^- into an octahedral $H_3O^+\text{–}O^-$ structure (Fig. 2), with concurrent production of a mobile electron. Furthermore, if the well-known Grotthuss mechanism for

hydrogen ion transport is operative in these systems, proton "diffusion" away from the reaction site would readily result in a hydrated O^- ion like Model O-I (Fig. 1).

Mechanism (6), on the other hand, supplies OH radicals from OH^- ionization, implying close proximity of two OH^- ions unless there is translational motion subsequent to the ionization step. The sequence as written could not take place within the first coordination sphere of a hydrated OH^-, and at least two such spheres would have to be involved. This situation, along with the statistical preponderance of water molecules in alkaline ice ($\sim 6H_2O$ per OH^- in 10 M NaOH), leads us to feel that mechanisms like (6), based on low energy ionization of OH^- ions, may be of relatively minor importance in O^- production.

The apparent consistency of our calculated O^- and OH^- results with mechanism (5) therefore prompts us to make the tentative suggestion that these reactions account for most of the production of O^- (and possibly of trapped electrons as well: the species are obtained in equal yields [2]) in alkaline ice irradiation, and that the octahedral H_3O^+–O^- and hydrated O^- models account for most of the stabilization of O^- ions so produced. (Schlick and Kevan have suggested [3] that there is an inhomogeneity in O^- sites in alkaline ice, so that two or more different types of sites may be involved in O^- stabilization.)

In any event, more definitive statements must await fairly detailed results concerning nearest neighbor interactions, particularly those involving spin, with the O^- ion. In that respect, our hydrated O^- results should be considered more reliable than those for the H_3O^+–O^- model. In fact, we have observed a tendency for interations to be exaggerated more by the INDO method as we went from anion–neutral molecule to anion–cation situations, and it is quite possible that a simple reparametrization of the INDO calculation might produce more useful quantitative results in these cases. The present work should therefore be considered a preliminary study, and we feel it has raised a number of points that deserve further development.

Acknowledgement is made to the University of Illinois at Chicago Circle Research Board for support of this research. The authors are grateful to the University of Illinois at Chicago Circle Computer Center for their generous donation of computer time. We also thank Mr. Arthur E. Stillman for his helpful comments and advice, and Professor Larry Kevan for readily sharing some of his experience and insight with us.

References

1. Kevan, L.: Radiation chemistry of frozen aqueous solutions, in: Radiation chemistry of aqueous systems, Stein, G., Ed. New York: Wiley-Interscience 1968
2. Kevan, L.: Radiation chemistry of frozen polar systems, in: Actions chimiques et biologiques des radiations, Vol. 13, Haissinsky, M., Ed. Paris: Masson 1969
3. Schlick, S., Kevan, L.: J. Phys. Chem. **81**, 1093 (1977)
4. Ershov, B. G., Puntezhis, S. A., Pikaev, A. K.: Khim. Vys. Energ. **5**, 185 (1971)
5. Schlick, S., Narayana, P. A., Kevan, L.: J. Chem. Phys. **64**, 3153 (1976)

6. Schuster, P.: Theory of hydrogen bonding in water and ion hydration, in: Structure of water and aqueous solutions (Proceedings of the International Symposium, Marburg 1973), Luck, W. A. P., Ed. Weinheim: Verlag Chemie 1974
7. Schuster, P., Jakubetz, W., Marius, W.: Topics in current chemistry, Vol. 60. Berlin: Springer-Verlag 1975
8. Pople, J. A., Beveridge, D. L.: Approximate molecular orbital theory. New York: McGraw-Hill 1970
9. Breitschwerdt, K. G., Kistenmacher, H.: Chem. Phys. Letters **14**, 288 (1972)
10. Cremaschi, P., Gamba, A., Simonetta, M.: Theoret. Chim. Acta (Berl.) **25**, 237 (1972)
11. Lischka, H., Plesser, Th., Schuster, P.: Chem. Phys. Letters **6**, 263 (1970)
12. Russeger, P., Lischka, H., Schuster, P.: Theoret. Chim. Acta (Berl.) **24**, 191 (1972)
13. Beurskens, G., Jeffrey, G. A.: J. Chem. Phys. **41**, 924 (1964)
14. Respectively QCPE 135 and QCPE 141, Quantum Chemistry Program Exchange, Indiana University, Bloomington, Indiana, USA
15. Fournier, M., Allavena, M., Potier, A.: Theoret. Chim. Acta (Berl.) **42**, 145 (1976)
16. Chesnut, D. B., Wormer, P. E. S.: Theoret. Chim. Acta (Berl.) **20**, 250 (1971)
17. Arshadi, M., Kebarle, P.: J. Phys. Chem. **74**, 1483 (1970)
18. Arshadi, M., Yamdagni, R., Kebarle, P.: J. Phys. Chem. **74**, 1475 (1970)
19. Kevan, L.: personal communication
20. Norgett, M. J., Stoneham, A. M., Pathak, A. P.: J. Phys. C: Solid State Phys. **10**, 555 (1977)

Received February 24, 1977/June 20, 1977